

# A New Model for Tensile Creep of Silicon Nitride

William E. Luecke<sup>\*,†</sup> and Sheldon M. Wiederhorn<sup>\*,‡</sup>

National Institute of Standards and Technology, Gaithersburg, Maryland 20899

The tensile creep rate of most commercial grades of Si<sub>3</sub>N<sub>4</sub> increases strongly with stress. Although the usual power-law functions can represent the creep data, the data often show curvature and systematic variations of slope with temperature and stress. In this article, we present a new approach to understanding the creep of ceramics, such as Si<sub>3</sub>N<sub>4</sub>, where a deformable second phase bonds a deformation-resistant major phase. A review of experimental data suggests that the rate of formation and growth of cavities in the second phase controls creep in these materials. The critical step for deformation is the redistribution of the second phase away from the cavitation site to the surrounding volume. The effective viscosity of the second phase and the density of active cavities determine the creep rate. Assuming that the hydrostatic stresses in pockets of the second phase are normally distributed leads to a model that accurately describes the tensile creep rate of grades of Si<sub>3</sub>N<sub>4</sub>. In this model, the creep rate increases exponentially with the applied stress, is independent of Si<sub>3</sub>N<sub>4</sub> grain size, is inversely proportional to the effective viscosity of the deformable phase, and is proportional to the cube of the volume fraction of the deformable phase.

## I. Introduction

RESEARCHERS have collected a substantial body of tensile creep data on commercial grades of Si<sub>3</sub>N<sub>4</sub>.<sup>1–6</sup> Most of them have summarized their creep data by the Norton equation:<sup>7</sup>

$$\dot{\epsilon}_s = \dot{\epsilon}_0 \left( \frac{\sigma}{\sigma_0} \right)^n \exp\left(-\frac{\Delta H}{RT}\right) \quad (1)$$

where  $\dot{\epsilon}_s$  is a secondary or minimum creep rate,  $\sigma$  the applied tensile stress,  $T$  the temperature in kelvin, and  $\dot{\epsilon}_0$ ,  $n$ , and  $H$  empirical constants of the fit. The stress exponent,  $n$ , and the activation enthalpy,  $H$ , are usually given a physical interpretation. Linear processes,  $n = 1$ , are usually interpreted as resulting from diffusional<sup>8–10</sup> or solution–precipitation<sup>11</sup> mechanisms. Quadratic processes,  $n = 2$ , usually result from interface–reaction–controlled diffusional mechanisms<sup>12–14</sup> or from linear mechanisms with a threshold stress.<sup>15</sup> More strongly nonlinear creep processes in metals and geologic ceramics, but not structural ceramics, for which  $n > 3$ , are usually interpreted as resulting from dislocation processes.<sup>16</sup>

Equation (1) often does not fit tensile creep data for Si<sub>3</sub>N<sub>4</sub> well. Recent studies on commercial Si<sub>3</sub>N<sub>4</sub><sup>§</sup> (NT154, Saint-Gobain/Norton Industrial Ceramics Corp., Northboro, MA;<sup>5,17</sup> SN-88, NGK Insulators, Ltd., Nagoya, Japan;<sup>18</sup> and AS800,

AlliedSignal, Torrance, CA<sup>19</sup>) have shown curvature in log(strain rate)–log(stress) plots. For some of these materials,  $n$  increases from  $\sim 2$  to as much as 5 (Ref. 5) or 6 (Ref. 18) with increasing stress. Because  $n$  varies, some authors have suggested that the mechanism of creep deformation differs at high and low stresses.<sup>3</sup> Other authors<sup>20</sup> have suggested that the Norton equation does not fit the creep data well, because deformation is not a consequence of creep mechanisms that lead to a power-law dependence on stress.

Gasdaska<sup>20</sup> suggested that a hyperbolic sine function of applied stress and temperature, which follows from Eyring's<sup>21</sup> theory of the viscosity of fluids, describes the tensile creep behavior better than does the Norton equation:

$$\dot{\epsilon}_s = A_s T \sinh\left(\frac{\Omega_s \sigma}{RT}\right) \exp\left(-\frac{\Delta H_s}{RT}\right) \quad (2)$$

where  $\Omega_s$  and  $\Delta H_s$  are the apparent activation volume and energy, respectively. For stresses greater than  $\sim 50$  MPa, Eq. (2) simplifies to an exponential function:

$$\dot{\epsilon}_s = A_s T \exp\left(\frac{-\Delta H_s + \Omega_s \sigma}{RT}\right) \quad (3)$$

Gasdaska attributed the rate-limiting step in the deformation process to sliding of Si<sub>3</sub>N<sub>4</sub> grains aided by the amorphous, siliceous layer separating them, and accommodated by diffusion and cavitation of the silicate phase, located at multigrain junctions. At high stresses, breakdown of the structure of the residual glass on Si<sub>3</sub>N<sub>4</sub> boundaries leads to shear thinning and a nonlinear dependence of creep rate on stress.

Li and Reidinger<sup>22</sup> applied Wakai's<sup>14</sup> step model of solution–precipitation creep to Si<sub>3</sub>N<sub>4</sub> to arrive at an inverse exponential form:

$$\dot{\epsilon}_s = A_{sm} \frac{\sigma^{2/3}}{T} \exp\left(-\frac{\Delta H_{sm}}{RT}\right) \exp\left(-\frac{L}{RT\sigma}\right) \quad (4)$$

where  $L$  is a term involving the height of the grain-boundary step on which Si<sub>3</sub>N<sub>4</sub> molecules are attaching and the energy of the step per unit length.

This article presents a new model for describing the tensile creep of ceramics. Although its focus is on Si<sub>3</sub>N<sub>4</sub>, the model applies in general to materials comprising a creep-resistant major phase bonded by a more easily deformed second phase.

Instead of a sliding process, we argue that the cavity formation in and subsequent redistribution of silicate phase limits the creep rate. We begin by summarizing the important experimental observations of the creep of Si<sub>3</sub>N<sub>4</sub>. We then discuss the limitations of a model for creep based on sliding of the Si<sub>3</sub>N<sub>4</sub> grains. Finally, we develop a model based on silicate redistribution and discuss its predictions and limitations.

## II. Summary of Experimental Observations and Inferences

### (I) Structure of Si<sub>3</sub>N<sub>4</sub>

Typically, liquid-phase-sintered Si<sub>3</sub>N<sub>4</sub> is made by adding small quantities of rare-earth oxides (e.g., Y<sub>2</sub>O<sub>3</sub>, Yb<sub>2</sub>O<sub>3</sub>, and

D. S. Wilkinson—contributing editor

Manuscript No. 190117. Received June 11, 1998; approved March 4, 1999.

<sup>\*</sup>Member, American Ceramic Society.

<sup>†</sup>Materials Science and Engineering Laboratory.

<sup>‡</sup>Ceramics Division.

<sup>§</sup>The use of commercial designations or company names is for identification only and does not indicate endorsement by the National Institute of Standards and Technology.

$\text{La}_2\text{O}_3$ ,  $\text{Al}_2\text{O}_3$ , or alkaline-earth oxides (e.g., SrO and MgO) to a fine-grained  $\alpha\text{-Si}_3\text{N}_4$  powder. These sintering aids react with the  $\text{SiO}_2$  present on the surface of the starting powder to form a low-melting glass that allows densification,  $\alpha\text{-Si}_3\text{N}_4$  to  $\beta\text{-Si}_3\text{N}_4$  transformation, and grain growth during hot-pressing, hot isostatic pressing (HIPing), and gas-pressure sintering. The final product comprises a network of elongated  $\beta\text{-Si}_3\text{N}_4$  grains, typically  $5\ \mu\text{m}$  long and  $1\ \mu\text{m}$  wide, whose interstices are filled with a mixture of submicrometer  $\beta\text{-Si}_3\text{N}_4$  grains and the residual silicate. These interstitial pockets of silicate are connected via triple-junction channels. An amorphous, siliceous phase,<sup>23–25</sup> usually  $\sim 1\text{--}2\ \text{nm}$  thick, separates the grains of  $\text{Si}_3\text{N}_4$ . This amorphous interfacial phase typically does not crystallize during processing or high-temperature exposure. In contrast, the sintering aid remaining at multigrain junctions, which forms its own interconnected network, usually can be crystallized to rare-earth silicate phases.

## (2) Experimental Observations

Numerous studies of creep of  $\text{Si}_3\text{N}_4$  have revealed common features:

(i)  $\text{Si}_3\text{N}_4$  creeps much faster in tension than in compression.<sup>5,20,26–32</sup> Figure 1 illustrates this behavior, where the logarithm of the minimum creep rate for several different silicon

nitrides is plotted as a function of the logarithm of the applied stress. At the same stress, the tensile creep rate is anywhere from 10 to 100 times greater than the compressive creep rate. At low stresses, extrapolations of the two curves converge. Asymmetric creep also occurs in siliconized  $\text{SiC}$ ,<sup>33</sup>  $\text{Al}_2\text{O}_3$ ,<sup>28</sup> and glass-ceramics.<sup>34</sup> All of these materials are composed of a deformation-resistant major phase ( $\text{Si}_3\text{N}_4$ ,  $\text{Al}_2\text{O}_3$ , or  $\text{SiC}$ ) and an easily deformed minor phase at the grain boundaries and multigrain junctions. In contrast, single-phase  $\text{Al}_2\text{O}_3$ <sup>35</sup> exhibits equal tension and compression creep rates.

(ii) Figure 2 shows that the curvature in the tensile creep rate of  $\text{Si}_3\text{N}_4$  evident in Fig. 1 is captured by expressing the creep rate as an exponential function of the applied stress and temperature. This behavior occurs in at least five grades of  $\text{Si}_3\text{N}_4$ .<sup>5,18–20,32,36,37</sup> In comparison, the compressive creep rate is a power-law function of the applied stress; values of  $n$  generally range from  $\sim 1$ <sup>5,27,28,30,38–47</sup> to  $\sim 2$ .<sup>39,40,48–51</sup>

(iii) Cavity formation produces the bulk of the tensile creep strain in  $\text{Si}_3\text{N}_4$ . In studies on seven different silicon nitrides (see Fig. 3),<sup>5,18–20,52–54</sup> the cavity volume fraction increases linearly with the tensile creep strain, with a slope ranging from  $\sim 0.8$  to 1. Although cavitation can also occur in compression,<sup>5,39,40</sup> the volume fraction of cavities is typically much less than that observed in tension<sup>5</sup> under similar stress

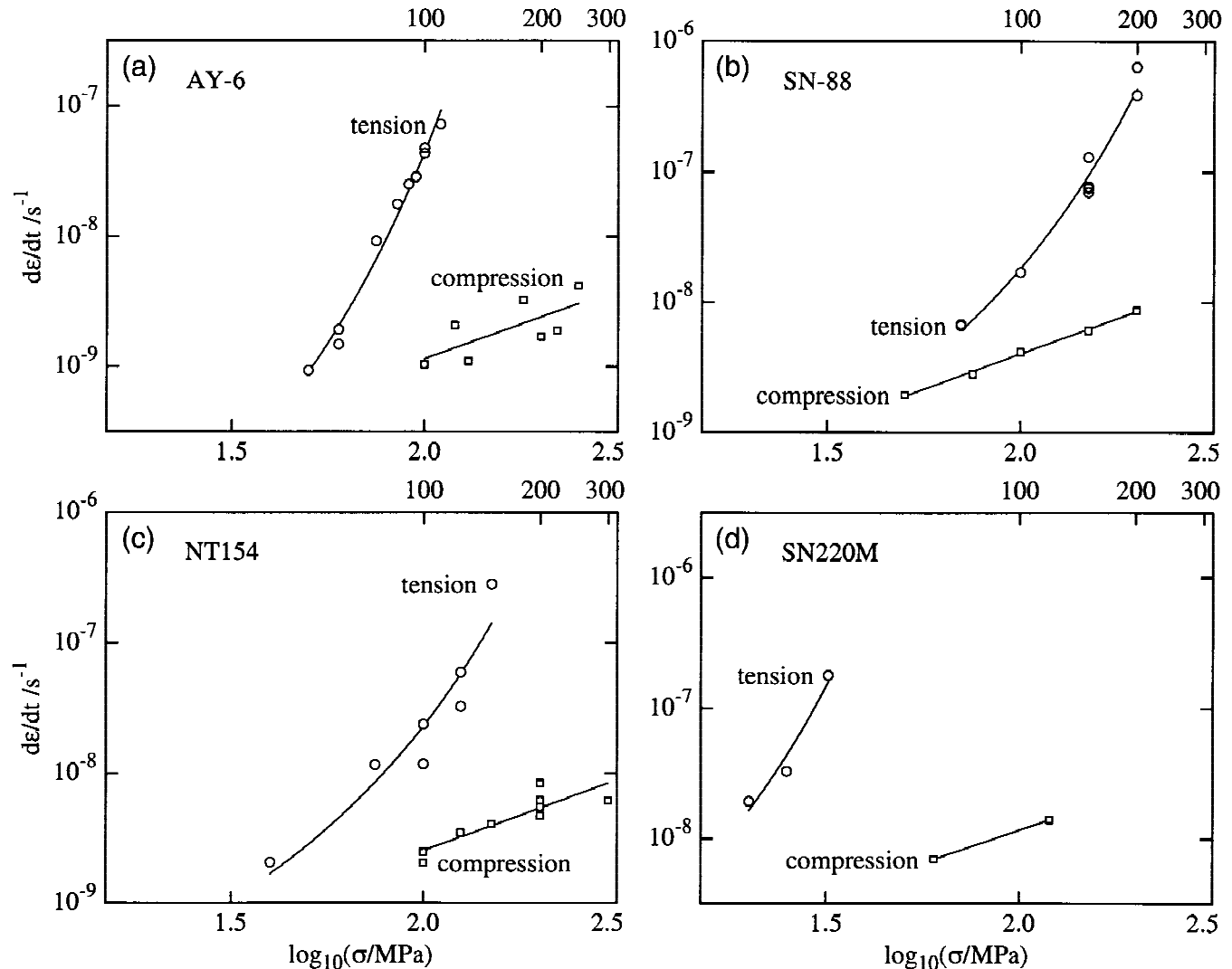


**Fig. 1.** Comparison of creep behavior of several silicon nitrides in tension and compression: (a) AY-6, a SiC-whisker-reinforced  $\text{Si}_3\text{N}_4$ <sup>27</sup> tested at  $1200^\circ\text{C}$ ; (b) SN-88, a gas-pressure-sintered  $\text{Si}_3\text{N}_4$ <sup>18</sup> tested at  $1400^\circ\text{C}$ ; (c) NT154, a HIPed  $\text{Si}_3\text{N}_4$ <sup>5</sup> tested at  $1430^\circ\text{C}$ ; and (d) SN220M, a sintered  $\text{Si}_3\text{N}_4$ <sup>28</sup> tested at  $1200^\circ\text{C}$ .

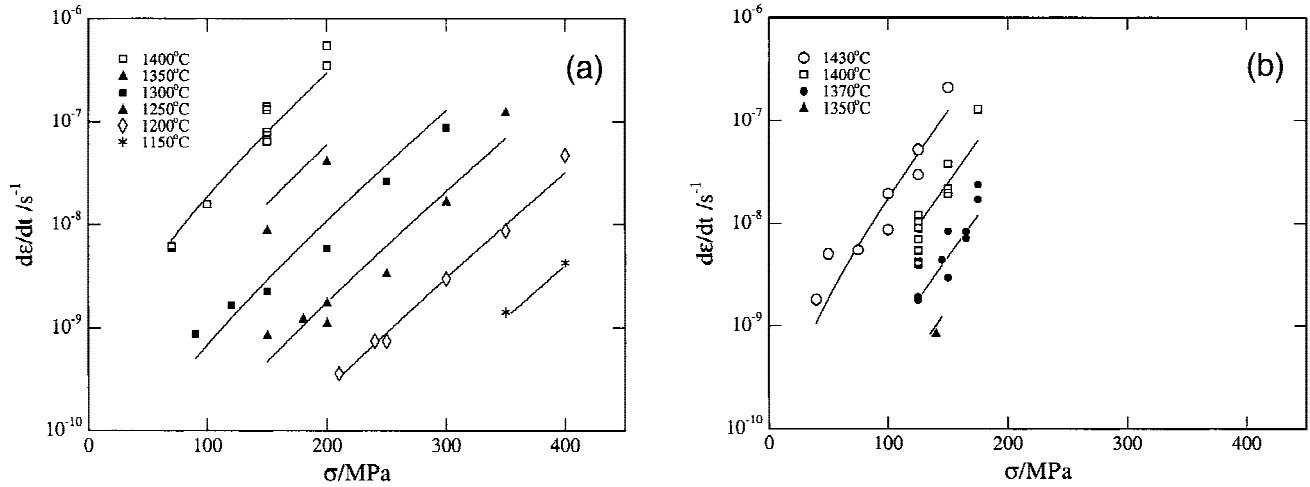


**Fig. 2.** Creep data for two silicon nitrides: (a) SN-88, a gas-pressure-sintered material<sup>18</sup> and (b) NT154, a HIPed material.<sup>36</sup> Solid lines are the fits to the data of a function (Eq. (20)) with an exponential stress dependence. Note that the stress axis is linear, rather than logarithmic.

and strain. When the stress exponent for compression creep is near unity, there is no cavitation.<sup>5,27,39-41,46,48,55</sup> Cavitation accompanies compression creep only in cases when  $n > 2$ .<sup>39-41</sup>

(iv) Cavities nucleate and grow primarily in the interstitial pockets of silicate located at multigrain junctions (see Fig. 4).<sup>5,17,20,22,56,57</sup> Once the silicate phase has completely left the pocket, the cavity stops growing.<sup>5</sup> A study using small-angle X-ray scattering has shown that the continuous addition of new cavities, rather than the growth of existing cavities, dominates the volume addition.<sup>5</sup> Although some studies<sup>2,5,6,17,58</sup> have

shown that Hull-Rimmer-style cavities<sup>59</sup> sometimes form on  $\text{Si}_3\text{N}_4$  grain boundaries, these interfacial cavities do not contribute greatly to the overall cavity volume.<sup>5</sup>

(v) Most experimental evidence suggests that dislocations are not active during tensile,<sup>5,26</sup> compression,<sup>40-42,46,48,55</sup> or flexural<sup>60</sup> creep. Even when dislocations are observed,<sup>22</sup> there appears to be no difference in dislocation structure between the as-received and the deformed material. Only rarely do researchers note a change in dislocation density<sup>61,62</sup> after creep.

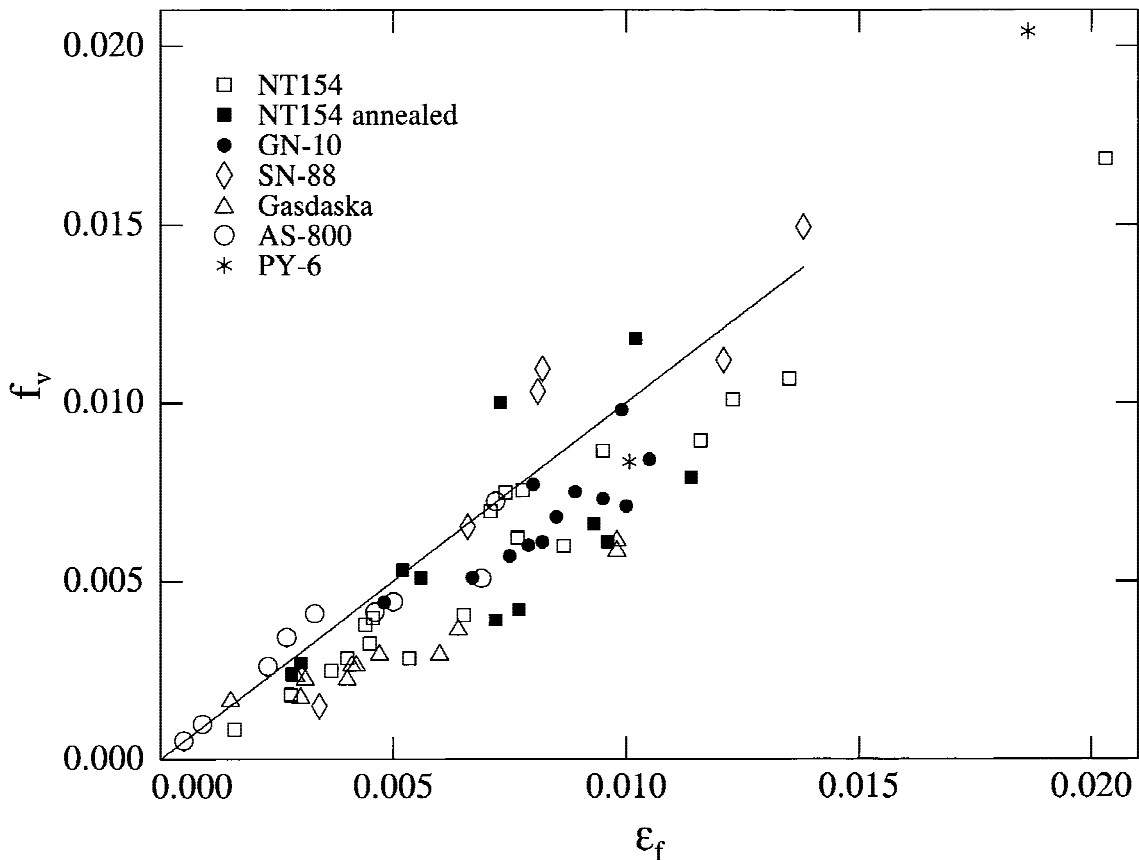


**Fig. 3.** Volume fraction of cavities as a function of strain for six silicon nitrides ((□) NT154, (■) NT154, annealed to produce larger grains,<sup>52</sup> (●) GN-10,<sup>53</sup> (◇) SN-88,<sup>18</sup> (△) Gasdaska's<sup>20</sup> experimental  $\text{Si}_3\text{N}_4$ , (○) AS-800,<sup>19</sup> and (\*) PY-6<sup>54</sup>). Volume fraction of cavities increases linearly with strain, independent of temperature. Solid line has a slope of unity.

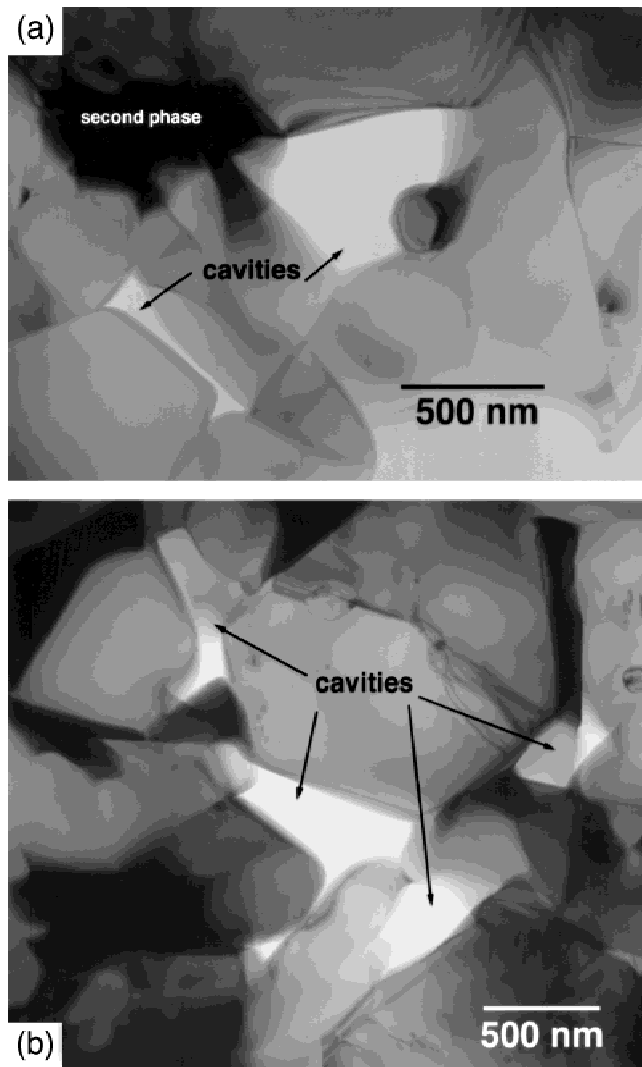


**Fig. 4.** Interstitial cavities in (a) NT154, a HIPed  $\text{Si}_3\text{N}_4$ ,<sup>5</sup> crept for 689 h at 1430°C under 75 MPa to a failure strain of 0.020, and (b) SN-88, a gas-pressure-sintered  $\text{Si}_3\text{N}_4$ ,<sup>18</sup> crept for 477 h at 1400°C under 100 MPa to a failure strain of 0.042. References 20 and 56 show micrographs of similar cavities in other silicon nitrides.

### (3) Inferences

The above observations lead to the following conclusions about possible creep mechanisms:

(i) The usually linear or parabolic dependence of compressive creep rate on stress and the existence of the nanometer-thick amorphous layers on two-grain boundaries are evidence that a diffusional creep mechanism on the boundaries,<sup>10</sup> such as solution-precipitation creep,<sup>11</sup> controls compressive creep.  $\text{Si}_3\text{N}_4$  dissolves from boundaries under compression, diffuses through the amorphous layer, and precipitates onto tensile boundaries.

(ii) Diffusional creep of  $\text{Si}_3\text{N}_4$  cannot contribute significantly to the tensile creep strain. Diffusional creep is symmetric in stress;<sup>8–10</sup> therefore, the creep rate in tension and compression would be equal if solution-precipitation of  $\text{Si}_3\text{N}_4$  controlled both creep processes. Because tensile creep can be as much as 100 times faster than compressive creep,<sup>5,20,26–28,63</sup> some other mechanism must produce the tensile creep deformation of  $\text{Si}_3\text{N}_4$ .

(iii) If neither diffusional transport of  $\text{Si}_3\text{N}_4$  nor dislocation motion within  $\text{Si}_3\text{N}_4$  grains occurs during tensile deformation, then there is no mechanism by which  $\text{Si}_3\text{N}_4$  grains can change their shape during deformation.<sup>5</sup> Therefore,  $\text{Si}_3\text{N}_4$  behaves as a granular solid, similar to a soil:<sup>64</sup> the grains of  $\text{Si}_3\text{N}_4$  are rigid

relative to the deformation process. Only the network of grains changes shape during deformation. Because of the close-packed nature of the grains, the network must dilate during the deformation process.<sup>65</sup>

(iv) The linear increase of cavity volume fraction with creep strain (Fig. 3) suggests that tensile creep of  $\text{Si}_3\text{N}_4$  is linked to the process of interstitial pocket cavitation. Stresses build up locally during the deformation process as a consequence of the applied stress and the relative motion of the grains. The formation of a cavity in an interstitial pocket relieves that stress, but the pocket remains connected to other stressed interstitial pockets via the triple-junction network. Silicate from the cavitated pocket must redistribute to surrounding pockets in response to this stress gradient.

## III. Model Development for Tensile Creep

### (1) Review of Cavitation Creep Models in Structural Ceramics

Researchers have long recognized the importance of cavities in the high-temperature rupture process in structural ceramics. Much of that cognition has gone into developing theories of the linkage of individual cavities into the macro-flaws whose ultimate extension causes failure, as a way to develop life-prediction models.<sup>66–69</sup> Most often, the focus of these models has been on the nature of the damage and not the resulting creep behavior. Other models have focused on the difficult and important question of the origin of the large stresses needed to nucleate cavities,<sup>66,70–72</sup> instead of predicting the overall creep rate of the loaded body. All of these aspects are certainly important in understanding creep rupture, but our focus is on the relation between the cavitation process and the resulting creep rate.

Few models have explicitly attempted to derive a form for the creep rate when cavities play an important role in the process. Evans and Rana,<sup>68</sup> as part of a life-prediction model for creep rupture of structural ceramics, have developed a model in which the creep strain results from the elastic opening of facet-sized microcracks.

Suresh and Brockenbrough<sup>73</sup> extended the model. Several experimental studies<sup>56,74</sup> have applied the model to  $\text{Si}_3\text{N}_4$  creep. Although the model does give power-law dependence of the creep rate on stress, the resulting elastic strains are very small, even for cracks (as opposed to cavities), and the possible strains are much smaller than the usual strains in creeping  $\text{Si}_3\text{N}_4$ .

Morrell and Ashbee<sup>34</sup> have developed a model for tensile creep of glass ceramics in which viscous flow of the intergranular phase produces the deformation. To explain the power-law dependence of strain rate on stress, they have postulated that cavitated regions shed load to uncavitated regions; the local deformation remains linear-viscous, but  $n$  can be  $\gg 1$ . Arons and Tien<sup>75</sup> and Kossowsky *et al.*<sup>26</sup> have applied the model to  $\text{Si}_3\text{N}_4$ , and Ferber and Jenkins<sup>6</sup> have promoted a model of similar form.

Lange<sup>76</sup> has developed a simple model for creep of  $\text{Si}_3\text{N}_4$  where he argues that deformation of the material by flow of the second phase on two-grain boundaries must proceed by the viscous growth of a cavity. Non-Newtonian creep of the body must result from non-Newtonian rheology of the two-grain boundary material. Typically, two-grain-boundary cavities, such as appear in Lange's model, do not occur in  $\text{Si}_3\text{N}_4$ , and the model neglects the effect of the constraint<sup>77</sup> of the surrounding uncavitated regions.

Dryden *et al.*<sup>78</sup> have developed and extended<sup>79,80</sup> a similar model for deformation by flow of the two-grain-boundary material. The model, which they have used to model the early stages of creep in  $\text{Si}_3\text{N}_4$ ,<sup>80,81</sup> does not explicitly involve cavitation but does seem to be a good candidate to rationalize the creep behavior at very small strains. As with Lange,<sup>76</sup> any non-Newtonian creep would have to result from the non-

Newtonian rheology of the two-grain-boundary material. Recently, Dey *et al.*<sup>82</sup> have developed a model for creep similar to Dryden *et al.*, but which incorporates the idea of load shedding of cavitated regions to noncavitated regions (à la Morrell and Ashbee<sup>34</sup>) to explain the nonlinearity of the overall creep deformation. Because the thickness of the amorphous, siliceous, two-grain boundaries in Si<sub>3</sub>N<sub>4</sub> is less than several nanometers,<sup>23–25</sup> this mechanism must cease after very small ( $\epsilon < 0.001$ ) strains.

These existing models for creep, with the exception of the model of Gasdaska<sup>20</sup> discussed in the Introduction, do not capture the behavior of Si<sub>3</sub>N<sub>4</sub> outlined in Section II(2). The inferences of Section II(3) suggest three possible rate-limiting steps for creep: cavity nucleation; Si<sub>3</sub>N<sub>4</sub> grain-boundary sliding as the structure dilates to accommodate the silicate redistribution; or flow of the silicate phase through the Si<sub>3</sub>N<sub>4</sub> network from the cavitating pocket. In an earlier paper, we concluded<sup>83</sup> that cavity nucleation could not be the rate-limiting step of the creep process. Classical nucleation theory predicts  $n > 10^4$  (in Eq. (1)), or much larger than the  $n$  values of  $3-10^{1.3, 6, 20, 27, 28, 75, 84-86}$  that current silicon nitrides exhibit. Therefore, in the remainder of this article, we examine only grain-boundary sliding or redistribution of the silicate phase from the cavity as possible rate-limiting steps for deformation. Both of these must occur during creep,<sup>5</sup> but the slower of the two controls the creep process.

Tensile deformation of Si<sub>3</sub>N<sub>4</sub> requires the redistribution of the second phase from cavities to the interstitial volume in the neighborhood of the cavity (Fig. 5). Because Si<sub>3</sub>N<sub>4</sub> is normally fully dense, there is no room for redistribution unless the network of Si<sub>3</sub>N<sub>4</sub> grains surrounding the cavity dilates to increase the interstitial volume to accommodate the silicate phase leaving the cavity. Without dilation, the surrounding, undeformed material exerts a back stress to constrain further cavity growth, a process that Dyson<sup>77</sup> first recognized. The volume increase caused by the dilation is equal to the volume of the cavity and occurs within a region defined by spacing between active cavities. Si<sub>3</sub>N<sub>4</sub> grain-boundary sliding accommodates the dilation. Because the redistribution of silicate takes place, in general, over a volume comprising many Si<sub>3</sub>N<sub>4</sub> grains, calculating the creep rate of the body requires calculating the creep rate of a volume of material encompassing a single cavity and the vol-

ume over which its silicate redistributes. For simplicity, consider this volume to be a cube with sides of length  $L$  (see Fig. 5). The spacing between active cavities is then also  $L$ .

Experimental observations have shown that cavitation during tensile creep of Si<sub>3</sub>N<sub>4</sub> produces strain primarily in the axial direction of the specimen, rather than uniform outward expansion. This is easily demonstrated from the following arguments.<sup>57</sup> The change in density,  $\Delta\rho/\rho$ , can be related to the principal components of strain:

$$-\frac{\Delta\rho}{\rho} = \frac{\Delta V}{V} = 2\epsilon_{33} + \epsilon_{11} \quad (5)$$

where  $\Delta V/V$  is the relative change in volume,  $\epsilon_{33}$  the lateral strain, and  $\epsilon_{11}$  the axial strain. For most silicon nitrides characterized,<sup>5, 18, 19, 53</sup>  $0.8 \epsilon_{11} < \Delta V/V < 1.1 \epsilon_{11}$ , yielding a lateral strain in the range  $0.1 > \epsilon_{33} > -0.05$ . Siliconized SiC<sup>87, 88</sup> behaves similarly. In only one study was the calculated lateral strain in the Si<sub>3</sub>N<sub>4</sub> larger than reported above; i.e.,  $\epsilon_{33} = 0.2$ .<sup>20</sup> For simplicity in the model development below, we assume that, during tensile deformation, the axial strain is equal to the volume fraction of cavities; i.e.,  $\Delta V/V = \epsilon_{11}$  and  $\epsilon_{33} = 0$ .

(2) Grain-Boundary Sliding as the Rate-Limiting Step for Creep

If grain-boundary sliding is the rate-limiting step for the creep process, we can imagine the cube of Si<sub>3</sub>N<sub>4</sub> surrounding the cavity to be crossed by many slip planes along which the deformation occurs (Fig. 6). If all grain boundaries slide, then the separation between planes,  $l$ , is the grain size; if groups of grains slide, then  $l$  is larger than the grain size. The resistance to intergranular sliding is then the resistance to sliding of the nanometer-thick, amorphous, siliceous layer that separates Si<sub>3</sub>N<sub>4</sub> grains.

Assume the amorphous, siliceous layer separating sliding Si<sub>3</sub>N<sub>4</sub> boundaries has thickness  $\delta$  and viscosity  $\eta$  and that sets of sliding boundaries lie a distance  $l$  apart, inclined to the loading axis at an angle  $\theta$  (Fig. 6). The shear stress,  $\tau$ , along a sliding boundary is  $\tau = \sigma \cos \theta \sin \theta$ . The shear strain rate,  $\dot{\gamma}$ , in the siliceous layer is  $\dot{\gamma} = \tau/\eta$ . The overall strain rate,  $\dot{\epsilon}$ , is then

$$\dot{\epsilon} = \frac{\delta \sigma}{l \eta} \sin^2 \theta \cos^2 \theta \quad (6)$$

For  $\theta = \pi/4$ , the plane that has the greatest shear stress,

$$\dot{\epsilon} = \frac{1}{4} \frac{\delta \sigma}{l \eta} \quad (7)$$

Equation (7) predicts that the strain rate increases linearly with stress, in contradiction to exponential-like dependence that actually occurs.<sup>5, 18, 20, 28</sup> Gasdaska<sup>20</sup> has suggested that the viscosity of the siliceous material at the grain boundaries may decrease with increasing applied stress and, thus, be responsible for the extreme sensitivity of the creep rate on stress.

Li and Uhlmann<sup>89</sup> first observed such non-Newtonian flow of a glass during fiber drawing of a homogeneous 0.08Rb<sub>2</sub>O-0.92SiO<sub>2</sub> glass at stresses >300 MPa. They used the Eyring<sup>21</sup> equation to fit their data:

$$\eta = \frac{\tau}{AT} \exp\left(\frac{E_0}{RT}\right) \sinh\left(-\frac{\tau V_0}{2RT}\right) \quad (8)$$

where  $A$  is a constant,  $\tau$  the shear stress,  $E_0$  the height of the potential barrier to flow, and  $V_0 = A_0 a_0$  the shear volume. In the Eyring formalism, the parameter  $A_0$  is the cross section of the molecule or other molecular unit of the glass undergoing slip and  $a_0$  the slip distance. The shear volume,  $V_0$ , obtained by fitting Eq. (8) to the viscous flow data was about 5 times larger than the molar volume of 28 cm<sup>3</sup>/mol of the glass.<sup>22</sup> Although Li and Uhlmann questioned how physically reasonable such a large shear volume might be, the Eyring theory does have the correct form to rationalize the creep data shown in Fig. 1.

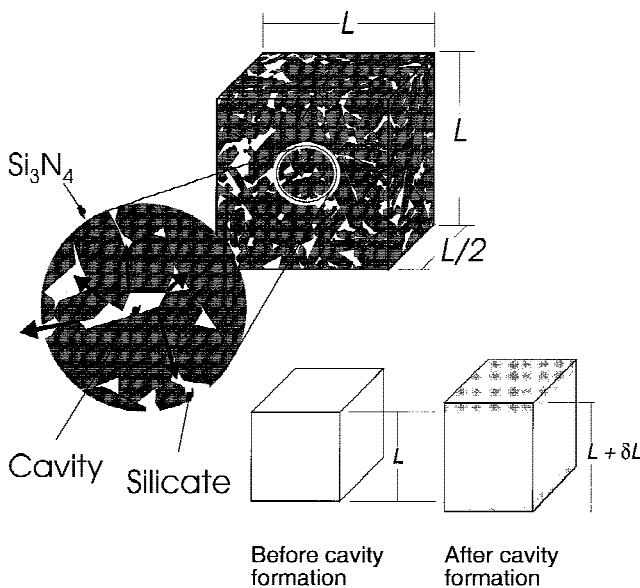
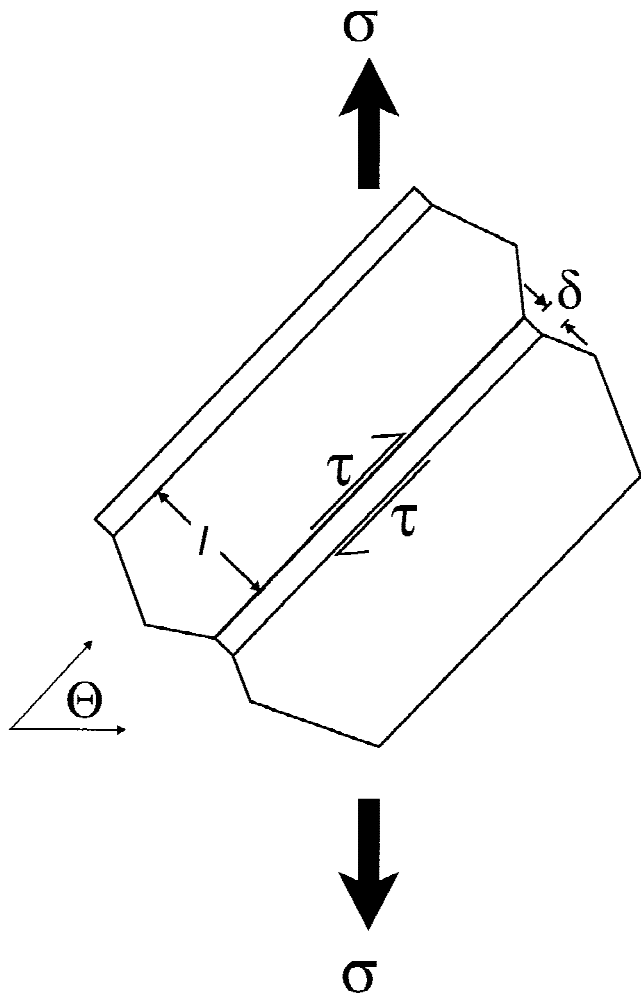


Fig. 5. Silicate phase from an interstitial cavity flows from the cavity through the triple-junction network to other interstitial pockets. Grain-boundary sliding of Si<sub>3</sub>N<sub>4</sub> accommodates the expansion of the interstitial pockets. Experimental evidence indicates that the strain produced is primarily axial.



**Fig. 6.** Model for sliding-limited creep. Model assumes that the creep rate is limited by the rate at which the grains can slide over one another as the material elongates. For simplicity, the sliding elements are assumed to lie at  $45^\circ$  to the applied stress, and the planes along which sliding occurs are spaced a distance  $l$  apart.

Substituting Eq. (8) for  $\eta$  into Eq. (7) gives an expression for the overall specimen creep rate:

$$\dot{\epsilon} = \frac{A \delta}{2 l} \exp\left(-\frac{\Delta H}{RT}\right) \sinh\left(-\frac{\sigma \Omega}{RT}\right) \quad (9)$$

where  $\Omega = V_0/4$  and  $\Delta H = E_0$ .

In the years since Li and Uhlmann's observation, there have been other observations of new-Newtonian flow in silicate glasses (see, for example, Webb's review<sup>90</sup>). Although a detailed atomistic description of the transition to non-Newtonian flow does not exist, all the silicates studied show the transition at viscosities whose relaxation times approach that of Si–O bond exchange.<sup>90</sup> The inverse of the Maxwell relation,

$$\dot{\epsilon}_R = \frac{G_\infty}{\eta} \quad (10)$$

defines a relaxation strain rate,  $\dot{\epsilon}_R$ , in terms of the viscosity and unrelaxed shear modulus,  $G_\infty$ . Silicate melts, regardless of composition,<sup>91</sup> deviate from Newtonian viscosity only at strain rates greater than  $\dot{\epsilon}_R/1000$ .

The best estimate of the strain rate of the interfacial amorphous silicate in creeping  $\text{Si}_3\text{N}_4$  is several thousand times less than this rate, even for the most relaxed assumptions about stress and composition. If we assume that the siliceous material on  $\text{Si}_3\text{N}_4$  grain boundaries behaves as a silicate glass, then we can estimate, using Eq. (7), its strain rate during creep to ascertain whether it might be expected to show nonlinear viscos-

ity. Consider the creep of NT154  $\text{Si}_3\text{N}_4$ <sup>5</sup> at  $1430^\circ\text{C}$  and 150 MPa, where the secondary creep rate is  $3.2 \times 10^{-7} \text{ s}^{-1}$ . This creep rate is almost the maximum observed for this material. In the neighborhood of these conditions,  $n \approx 8$ , placing the material well into the non-Newtonian regime. The thickness,  $\delta$ , of the amorphous, siliceous layer is  $\sim 1 \text{ nm}$ ,<sup>5,17</sup> and the grain size,  $l$ , is  $\sim 1 \mu\text{m}$ .<sup>5,17</sup> From Eq. (7), an upper-bound estimate for the strain rate of the interfacial amorphous layer is  $(l/\delta)\dot{\epsilon} = 3.2 \times 10^{-4} \text{ s}^{-1}$ . The corresponding relaxation strain rate for pure silica-glass, which is perhaps the most viscous of glasses and certainly much more viscous than the impurity-laden glass actually present on the boundaries, is  $206 \text{ s}^{-1}$ , assuming an unrelaxed shear modulus of 43 GPa<sup>92</sup> and viscosity,  $\eta$ , of  $2.08 \times 10^8 \text{ Pa}\cdot\text{s}$ .<sup>93</sup> The viscosity of pure silica, then, should only just begin to deviate from linearity at rates of  $\sim 0.2 \text{ s}^{-1}$ , or 1000 times faster than the fastest possible strain rate observed in practice. The presence of any of the sintering cations should significantly reduce the viscosity of the interfacial glass, with a concomitant increase of the relaxation rate. Based on the current understanding of the phenomenology of nonlinear viscosity in silicate glass, the interfacial amorphous silicate is not a likely source of the exponential increase of tensile creep rate with stress in  $\text{Si}_3\text{N}_4$ .

### (3) Redistribution of Silicate as the Rate-Limiting Step for Creep

Because the possibility of nonlinear viscosity of the amorphous, siliceous material on the  $\text{Si}_3\text{N}_4$  grain boundaries does not seem to be a good candidate for explaining the exponential dependence of tensile creep rate on stress, we now turn to the redistribution step as a possible rate-limiting mechanism. If the redistribution of the silicate through the intergranular channels controls the creep rate, then the size and spacing of channels, the effective viscosity of the silicate phase, and the spacing of the cavities are the important factors that must be considered in developing a creep model. Engineers and geologists interested in the flow of fluids through packed beds have treated this problem by generalizing the Hagen–Poiseuille equation for viscous flow through a narrow tube<sup>94–96</sup> by substituting a hydraulic radius for the radius of the tube. The hydraulic radius is defined as the ratio of the cross-sectional area of the bed available for flow to its wetted perimeter.<sup>97</sup> The Carman–Kozeny equation<sup>97,98</sup> relates the superficial velocity (i.e., at the entrance to the bed) of a fluid,  $v_0$ , of effective viscosity  $\eta$ , to the decrease in pressure  $\Delta P$ , across a bed of length  $L$ , packed with particles of mean diameter  $D$ , with volume fraction of voids  $\Phi$ :

$$v_0 = \frac{1}{k_0} \frac{\Delta P D^2}{L \eta (1 - \Phi)^2} \quad (11)$$

where  $k_0$  is a geometrical term. Because it is the silicate phase that is transported during tensile creep,  $\Phi$  refers the volume fraction of silicate rather than the volume fraction of cavities. The viscosity,  $\eta$ , is really an effective viscosity that describes the temperature dependence of the deformation of the crystalline silicate phase. It is not the viscosity of the interfacial amorphous silicate.

Equation (11) is the basis for the creep-rate model. As the silicate phase leaves the cavity and flows through the intergranular network of silicate channels, the network of  $\text{Si}_3\text{N}_4$  grains dilates to accommodate the increase in volume. Flow occurs on a local scale; the silicate phase from each cavity flows no more than one-half the distance between cavities. In accord with the experimentally observed volume changes,<sup>5,18–20,52–54</sup> we assume that flow occurs primarily in the direction of loading. Silicate phase from the cavity flows into a volume of the specimen defined by a box  $L$  on a side (Fig. 5). As the silicate flows from the cavity, the volume increases in length at a rate  $v_0$  to accommodate the silicate phase, yielding an overall creep rate of  $\dot{\epsilon} = v_0/L$ . Once a cavity forms, the stress within the interstitial pocket is almost zero, while the stress on the end of the box that surrounds the cavity is equal to the applied stress,  $\sigma$ . The term  $\Delta P$  in Eq. (11) can

be replaced by the hydrostatic stress,  $\sigma_h = \sigma/3$ . These substitutions transform Eq. (11) to

$$\dot{\epsilon} = \frac{\sigma}{3k_0\eta} \left(\frac{D}{L}\right)^2 \frac{\Phi^3}{(1-\Phi)^2} \quad (12)$$

where the creep rate depends on the applied stress,  $\sigma$ , the effective viscosity of the silicate phase,  $\eta$ , the grain size,  $D$ , the distance between cavities,  $L$ , and the volume fraction of silicate phase,  $\Phi$ .

As with the model for sliding (Eq. (7)), the linear stress dependence for the strain rate predicted by the flow-limited model (Eq. (12)) is in conflict with observed exponential stress dependence for  $\text{Si}_3\text{N}_4$ . For the model to be consistent with the creep behavior, other variables in Eq. (12) must also depend on stress, i.e.,  $\eta$  or  $L$ . In this section we show that the stress dependence of the creep rate can be correctly predicted by assuming that the spacing,  $L$ , between actively growing cavities decreases with increasing stress. Although the model is largely phenomenological, it yields an exponential dependence of creep rate on applied stress, in agreement with experimental data.

The applied load stresses each interstitial silicate pocket to a different magnitude, depending on the local configuration of the grains. The stress in some silicate pockets is large enough to nucleate cavities, while in others it is almost zero. Measurements of residual tensile and compressive stresses >1 GPa in cermet<sup>99,100</sup> support this assumption. Cavity nucleation also certainly requires such high stresses, which the applied load must generate.

There are many choices for the shape of the distribution of stresses in the interstitial pockets. Theoretical calculations of residual stresses resulting from thermal expansion anisotropy<sup>101</sup> predict that the stresses should be normally distributed. In the derivation that follows, we assume that the hydrostatic stress in the pockets,  $\sigma_h$ , follows a normal distribution with a mean stress,  $\sigma_\mu$ , proportional to the applied stress ( $\sigma_\mu = \sigma/3$ ) and constant standard deviation,  $s$ . A cavity nucleates in an interstitial pocket when its hydrostatic stress exceeds a critical value,  $\sigma_c$ . The fraction of interstitial pockets with stress greater than the critical stress for cavity nucleation is the area of the upper tail of the normal distribution:

$$Q(x) = 1 - \frac{1}{\sqrt{2\pi}} \int_{-\infty}^x e^{-t^2/2} dt \quad (13)$$

where  $x \equiv (\sigma_c - \sigma_\mu)/s$ . For any close packing of grains, there is about one interstitial pocket per grain; therefore, the number of interstitial pockets per unit volume,  $N_v$ , with  $\sigma_h > \sigma_c$  is

$$N_v(x) = \frac{Q(x)}{D^3} = \frac{1}{D^3} \left( 1 - \frac{1}{\sqrt{2\pi}} \int_{-\infty}^x e^{-t^2/2} dt \right) \quad (14)$$

An increase in applied stress shifts the entire distribution to higher stresses; i.e.,  $\sigma_\mu$  increases as the applied stress increases. The area under the tail of the distribution curve increases, and a greater fraction of pockets is cavitated.

Calculating the instantaneous creep rate, then, amounts to calculating the distance between active cavities and substituting the result into the expression for the strain rate (Eq. (12)). The distance  $L$  between active cavities is simply the inverse cube root of the number per unit volume:

$$L = Q(x)^{-1/3} D \quad (15)$$

Substituting the expression for  $L$  (Eq. (15)) into the expression for the creep rate (Eq. (12)) yields an expression for the creep rate:

$$\dot{\epsilon}_s = \frac{1}{3k_0} \frac{\sigma}{\eta} \frac{\Phi^3}{(1-\Phi)^2} Q(x)^{2/3} \quad (16)$$

from which the grain size,  $D$ , has dropped out.

Although we assume that the stress distribution function is constant in time, stresses within the specimen change both spatially and temporally as the specimen is deformed. Stress concentrations build up locally as a consequence of grain-boundary sliding. As the stress within a pocket reaches the critical stress,  $\sigma_c$ , a cavity forms, decreasing the local stress to a value that is determined by the surface tension,  $\gamma$ , of the silicate phase and the effective radius,  $r$ , of the cavity ( $\sigma = \gamma/r \approx 1$  MPa for a 1  $\mu\text{m}$  cavity). The fraction of the applied stress that was formerly carried by the silicate pocket is redistributed to other locations, which creates new stress concentrations and promotes continuous cavitation.

Evaluation of the creep rate,  $\dot{\epsilon}_s$ , requires the evaluation of  $Q(x)$  from the normal probability density function. Unfortunately, there is no closed-form solution for the integral of this function. However, for  $x > 1.4$ , the tail of the distribution can be approximated by<sup>102</sup>

$$Q(x) = \frac{(4+x^2)^{1/2} - x}{2} \frac{1}{\sqrt{2\pi}} \exp\left(-\frac{x^2}{2}\right) \quad (17)$$

For  $x > 3$ , the terms before the exponential are almost constant with  $x$ ; therefore,

$$Q(x) \approx \beta \exp\left(-\frac{x^2}{2}\right) \quad (18)$$

Assuming that the effective viscosity follows an Arrhenius form and substituting for  $Q(x)$  into Eq. (16) yields an expression for the creep rate as a function of stress and temperature:

$$\dot{\epsilon}_s = \frac{\beta^{2/3}}{3k_0} \frac{\sigma}{\eta_0} \exp\left(-\frac{\Delta H}{RT}\right) \frac{\Phi^3}{(1-\Phi)^2} \exp\left[-\frac{(\sigma_c - \sigma/3)^2}{3s^2}\right] \quad (19)$$

We have not been successful at evaluating all four independent parameters in Eq. (19) ( $\Delta H$ ,  $\sigma_c$ ,  $s$ , and the constant term). Because the experimental data lie so far from the critical stress,  $\sigma_c$ , and the curvature associated with the squared term in the exponential is so small, the uncertainties associated with  $\sigma_c$  and  $s$  are larger than their values. For the purposes of representing creep data, it is useful to further simplify Eq. (19). Expanding the stress term in the exponential, realizing that

$$\frac{2\sigma_c\sigma}{9\sigma^2} \gg \frac{\sigma^2}{27\sigma^2}$$

and deleting the constant  $-\sigma_c^2/3\sigma^2$  term from the exponential function transforms Eq. (19) to a simpler form that can be used to represent creep data:

$$\dot{\epsilon}_s = A\sigma \exp\left(-\frac{\Delta H}{RT}\right) \frac{\Phi^3}{(1-\Phi)^2} \exp(\alpha\sigma) \quad (20)$$

where

$$\alpha \approx \frac{2\sigma_c}{9\sigma^2}$$

and  $A$  contains all the constant terms. If the volume fraction of silicate,  $\Phi$ , is constant or unknown, it, too, can be included in the constant term,  $A$ . Figure 2 shows that Eq. (20) captures the curvature inherent in the creep data for  $\text{Si}_3\text{N}_4$ .

#### (4) Predictions of the Model

Equation (19) separates the stress, temperature, and microstructure dependence of the creep rate into discrete components. The temperature dependence of creep rate is entirely contained within the effective viscosity (or diffusivity) of the intergranular silicate phase. The apparent activation energy for creep of  $\text{Si}_3\text{N}_4$ , then, should equal the activation energy for deformation of the silicate phase. Although we have retained

the “viscosity” term in Eq. (19) for congruence with the flow model, the deformation of the silicate may occur by dislocation creep, dissolution of silicate into the interfacial, amorphous layer followed by reprecipitation in neighboring interstitial pockets, or by many other mechanisms. It is possible, however, that the critical stress for cavity formation,  $\sigma_c$ , may depend on temperature. If this is the case, then the apparent activation energy for creep no longer represents that for deformation of the silicate phase.

The derivation of Eq. (19) assumes that the microstructure has an inexhaustible supply of sites for cavitation and that creep continuously rearranges the microstructure so that the stress distribution on the interstitial sites remains temporally constant, although the stress on an individual interstitial pocket may change with time. That assumption allows us to calculate the instantaneous creep rate and equate it to the material creep rate. In practice, however, cavitation during creep may exhaust the supply of available sites as the cavity-prone sites are consumed. In this case, the creep rate decreases with increasing strain, as many have observed for  $\text{Si}_3\text{N}_4$ .<sup>1–3,5,6,18,20,22,26,27,56,75</sup> Alternatively,  $\text{Si}_3\text{N}_4$  grain contact may impede the sliding that accommodates the redistribution of silicate material and carry part of the load that the silicate pockets originally carried, in effect changing the stress distribution. Hirano *et al.*<sup>58</sup> have attributed the thousand-fold increase in tensile creep resistance of a  $\text{Si}_3\text{N}_4/\text{SiC}$  “nanocomposite” to suppression of grain-boundary sliding by submicrometer-sized SiC particles on grain boundaries. Transmission electron microscopy (TEM) investigations of  $\text{Si}_3\text{N}_4$  crept in tension,<sup>22,31</sup> compression,<sup>39–42,50,55</sup> and flexure<sup>60,103</sup> have often showed “strain whorls” caused by large elastic stresses at  $\text{Si}_3\text{N}_4$  grain contacts. In this case, the interstitial pockets do not experience the complete load, leading to a smaller fraction of them able to cavitate.

Equation (19) also predicts that the creep rate does not explicitly depend on the  $\text{Si}_3\text{N}_4$  grain size. There has been little systematic study of the grain-size dependence of the tensile creep rate in  $\text{Si}_3\text{N}_4$ , and the results to date are contradictory. Haig *et al.*<sup>86,104,105</sup> and Whalen *et al.*<sup>50</sup> produced grain size variants of a  $\text{Y}_2\text{O}_3\text{—MgAl}_2\text{O}_4$ -based  $\text{Si}_3\text{N}_4$ . In compression,<sup>50</sup> the large-grained material crept 30 times more slowly than a finer-grained material, in which the grains were roughly one-fifth as large. Preliminary experiments in tension<sup>86</sup> on a one- and coarse-grained material prepared from different billets of material indicated better creep resistance for the coarse-grained material. However, a more complete study, in which Haig *et al.*<sup>105</sup> prepared the coarse-grained material by further annealing of one-half of the billet that supplied the one-grained material, indicated no statistically significant difference in the tensile creep rates between the two grain sizes. French *et al.*<sup>106</sup> tested a  $\text{Yb}_2\text{O}_3$ -based  $\text{Si}_3\text{N}_4$ <sup>107,108</sup> in which the large-grained material was also prepared by long-term annealing of a small-grained, sintered starting material. The large-grained material, which had a microstructural scale  $\sim 4$  times that of the fine-grained material, crept faster than the one-grained material. In compression, however, the large-grained material crept more slowly than the small-grained material, as expected. Luecke and Wallace<sup>52</sup> prepared materials of various grain sizes based on a commercial HIPed  $\text{Si}_3\text{N}_4$  (NT154, Norton Co., Northboro, MA).<sup>5</sup> Although the interspecimen scatter was large, the largest-grained material crept faster in tension than the small-grained materials. Unlike the previous two studies, however, annealing the base material to promote grain growth did not result in significantly larger grains. Instead, with increased annealing time, the fine fraction of grains disappeared, but the largest grains did not grow significantly.

These seemingly contradictory results can be understood in light of the model in several ways. First, the act of annealing the materials at high temperature to promote  $\text{Si}_3\text{N}_4$  grain growth may have changed the impurity and/or second-phase distribution. In other words, besides changing the grain distribution, the anneal also may have changed the deformability ( $\eta$  in Eq. (19)) of the silicate phase. In this sense, the observed

change in creep behavior with increasing grain size is an artifact, rather than a real correlation. Second, the derivation of the creep equation implicitly assumes that the size and tortuosity of the channels through which the silicate must flow during creep is uniquely related to the grain size of the  $\text{Si}_3\text{N}_4$  through  $k_0$ . If grain growth alters this relation, then the model does not capture the grain-size dependence of the creep. Third, changing the grain-size distribution also undoubtedly changes the distribution of stresses in the interstitial pockets. In the formalism of Eq. (19), this amounts to changing either or both  $\sigma_c$  or  $s$ . It is even possible that changing the grain-size distribution might introduce a multimodal distribution of stresses in the interstitial pockets, further complicating the analysis.

The model predicts an almost cube dependence on the second-phase fraction. Given the difficulty in assessing the effect of  $\text{Si}_3\text{N}_4$  grain size on creep without introducing artifacts, it seems equally difficult to test this prediction.

Until this point, we have assumed that the cavitation mechanism is the only one that produces strain. Figure 1 indicates that the tensile and compressive creep rates converge at low stresses. If diffusional creep of  $\text{Si}_3\text{N}_4$  does control the compressive creep rate, then, at very low stresses, it may dominate the tensile creep rate as well. In this case, it is necessary to add a term that expresses the contribution of solution-precipitation creep to the overall rate (Eq. (19)). For very small strains, it is also necessary to include the contribution of the anelastic strains, which can range up to several tenths of percent.<sup>5,20,104,105,109</sup>

#### IV. Summary

This paper is an analysis of the tensile creep of  $\text{Si}_3\text{N}_4$ . Tensile creep data from many silicon nitrides support the idea that  $\text{Si}_3\text{N}_4$  deforms by the formation of cavities in the silicate-filled multigrain pockets that lie at the interstices of the  $\text{Si}_3\text{N}_4$  grains. As these cavities grow, the silicate phase flows through the network of triple junctions of  $\text{Si}_3\text{N}_4$  grains to other pockets. Dilation of the network of  $\text{Si}_3\text{N}_4$  grains accommodates the volume of the silicate phase displaced by the cavity formation. An analysis of the deformation based on the Carman–Kozeny equation, which describes the flow of fluids through packed beds, leads to a model for tensile creep that depends exponentially on applied stress. The effective viscosity of the silicate phase determines the temperature dependence of the creep rate, whereas the cavity spacing determines the stress dependence. The hydrostatic stresses within the silicate pockets,  $\sigma_h$ , are assumed to be normally distributed about a mean hydrostatic stress,  $\sigma_\mu$ . Above a critical hydrostatic stress,  $\sigma_c$ , cavities form; the number of cavities depends on the portion of the probability distribution curve that lies above a critical stress for cavitation. Increasing the applied stress shifts the distribution of interstitial pocket stresses to higher stresses, forming more cavities. This model naturally leads to an exponential dependence of creep rate on applied stress, and is consistent with the observed asymmetry in tensile and compressive creep rates, the formation of cavities only in tension, and the linear increase of cavity volume fraction with strain.

**Acknowledgment:** We thank Bernard Hockey for supplying the micrographs in Fig. 4.

#### References

1. J.-L. Ding, K. C. Liu, K. L. More, and C. R. Brinkman, “Creep and Creep Rupture of an Advanced Silicon Nitride Ceramic,” *J. Am. Ceram. Soc.*, **77**, 867–74 (1994).
2. M. K. Ferber, M. G. Jenkins, T. A. Nolan, and R. L. Yeckley, “Comparison of the Creep and Creep Rupture Performance of Two HIPed Silicon Nitride Ceramics,” *J. Am. Ceram. Soc.*, **77** [3] 657–65 (1994).
3. M. N. Menon, H. T. Fang, D. C. Wu, M. G. Jenkins, and M. K. Ferber, “Creep and Stress Rupture Behavior of an Advanced Silicon Nitride: II, Creep Rate Behavior,” *J. Am. Ceram. Soc.*, **77**, 1228–34 (1994).
4. S. M. Wiederhorn, G. D. Quinn, and R. F. Krause Jr., “Fracture Mechanism Maps: Their Applicability to Silicon Nitride”; p. 3661 in *Life Prediction Meth-*

ologies and Data for Ceramic Materials, ASTM STP 1201. Edited by C. R. Brinkman and S. F. Duffy. American Society for Testing and Materials, West Conshohocken, PA, 1994.

<sup>5</sup>W. E. Luecke, S. M. Wiederhorn, B. J. Hockey, G. G. Long, and R. F. Krause Jr., "Cavitation Contributes Substantially to Creep in Silicon Nitride," *J. Am. Ceram. Soc.*, **78** [8] 2085-96 (1995).

<sup>6</sup>M. K. Ferber and M. J. Jenkins, "Evaluation of the Strength and Creep-Fatigue Behavior of Hot Isostatically Pressed Silicon Nitride," *J. Am. Ceram. Soc.*, **75**, 2453-62 (1992).

<sup>7</sup>F. H. Norton, *The Creep of Steel at High Temperatures*. McGraw-Hill, New York, 1929.

<sup>8</sup>F. R. N. Nabarro, "Deformation of Crystals by the Motion of Single Ions"; pp. 75-90 in *Report of a Conference on Strength of Solids* (H. H. Wills Physical Laboratory, University of Bristol, July 7-9, 1947). Physical Society, London, U.K., 1948.

<sup>9</sup>C. Herring, "Diffusional Viscosity of a Polycrystalline Solid," *J. Appl. Phys.*, **21**, 437-45 (1950).

<sup>10</sup>R. L. Coble, "A Model for Boundary Diffusion Controlled Creep in Polycrystalline Materials," *J. Appl. Phys.*, **34** [6] 1679-82 (1963).

<sup>11</sup>R. Raj and C. K. Chyung, "Solution-Precipitation Creep in Glass Ceramics," *Acta Metall.*, **29**, 159-66 (1981).

<sup>12</sup>B. Burton, "Interface Reaction Controlled Creep: A Consideration of Grain-Boundary Dislocation Climb Sources," *Mater. Sci. Eng.*, **10**, 914 (1972).

<sup>13</sup>M. F. Ashby and R. A. Verrall, "Diffusion-Accommodated Flow and Superplasticity," *Acta Metall.*, **21**, 149-63 (1973).

<sup>14</sup>F. Wakai, "Step Model of Solution-Precipitation Creep," *Acta Metall. Mater.*, **42** [4] 1163-72 (1994).

<sup>15</sup>M. F. Ashby, "On Interface-Reaction Control of Nabarro-Herring Creep and Sintering," *Ser. Metall.*, **3**, 837-42 (1969).

<sup>16</sup>J.-P. Poirier, *Creep of Crystals*. Cambridge University Press, Cambridge, U.K., 1985.

<sup>17</sup>M. N. Menon, H. T. Fang, D. C. Wu, M. G. Jenkins, M. K. Ferber, K. L. More, C. R. Hubbard, and T. A. Nolan, "Creep and Stress Rupture Behavior of an Advanced Silicon Nitride: I, Experimental Observations," *J. Am. Ceram. Soc.*, **77**, 1217-27 (1994).

<sup>18</sup>R. F. Krause Jr., W. E. Luecke, S. M. Wiederhorn, J. D. French, and B. J. Hockey, "Tensile Creep and Rupture of Silicon Nitride," *J. Am. Ceram. Soc.*, **82** [5] 1233-41 (1999).

<sup>19</sup>H. A. Maupas; personal communication on creep of AlliedSignal AS800 Silicon Nitride, 1998.

<sup>20</sup>C. J. Gasdaska, "Tensile Creep in an *In Situ*-Reinforced Silicon Nitride," *J. Am. Ceram. Soc.*, **77**, 2408-18 (1994).

<sup>21</sup>H. Eyring, "Viscosity, Plasticity, and Diffusion as Examples of Absolute Reaction Rates," *J. Chem. Phys.*, **4**, 286-91 (1936).

<sup>22</sup>C.-W. Li and F. Reidinger, "Microstructure and Tensile Creep Mechanisms of an *In Situ*-Reinforced Silicon Nitride," *Acta Mater.*, **45** [1] 407-21 (1997).

<sup>23</sup>D. R. Clarke and G. Thomas, "Grain Boundary Phases in a Hot-Pressed MgO Fluxed Silicon Nitride," *J. Am. Ceram. Soc.*, **60**, 491-95 (1977).

<sup>24</sup>D. R. Clarke, "On the Equilibrium Thickness of Intergranular Glass Phases in Ceramic Materials," *J. Am. Ceram. Soc.*, **70**, 15-22 (1987).

<sup>25</sup>H.-J. Kleebe, "Structure and Chemistry of Interfaces in Si<sub>3</sub>N<sub>4</sub> Ceramics Studied by Transmission Electron Microscopy," *J. Ceram. Soc. Jpn.*, **105** [6] 453-75 (1997).

<sup>26</sup>R. Kossowsky, D. G. Miller, and E. S. Diaz, "Tensile and Creep Strengths of Hot-Pressed Si<sub>3</sub>N<sub>4</sub>," *J. Mater. Sci.*, **10**, 983-97 (1975).

<sup>27</sup>B. J. Hockey, S. M. Wiederhorn, W. Liu, J. G. Baldoni, and S.-T. Buljan, "Tensile Creep of Whisker-Reinforced Silicon Nitride," *J. Mater. Sci.*, **26**, 3931-39 (1991).

<sup>28</sup>M. K. Ferber, M. G. Jenkins, and V. J. Tennery, "Comparison of Tension, Compression, and Flexure Creep for Alumina and Silicon Nitride Ceramics," *Ceram. Eng. Sci. Proc.*, **11** [7-8] 1028-45 (1990).

<sup>29</sup>K. C. Liu, C. O. Stevens, C. R. Brinkman, and N. E. Holshausner, "A Technique to Achieve Uniform Stress Distribution in Compressive Creep Testing of Advanced Ceramics at High Temperatures," *J. Eng. Gas Turbines Power*, **119**, 500-505 (1997).

<sup>30</sup>A. A. Wereszczak, T. P. Kirkland, H.-T. Lin, and M. K. Ferber, "Tensile Creep Performance of a Developmental, *In Situ*-Reinforced Silicon Nitride," *Ceram. Eng. Sci. Proc.*, **18** [4] 45-55 (1997).

<sup>31</sup>F. Lofaj, H. Usami, A. Okada, and H. Kawamoto, "Long-Term Creep Damage Development in a Self-Reinforced Silicon Nitride"; pp. 337-52 in *Engineering Ceramics '96: Higher Reliability through Processing*. Edited by G. N. Babini et al. Kluwer, Dordrecht, The Netherlands, 1997.

<sup>32</sup>A. A. Wereszczak, M. K. Ferber, T. P. Kirkland, E. L. Frome, and M. N. Menon, "Asymmetric Tensile and Compressive Creep Deformation of Hot-Isostatically-Pressed Y<sub>2</sub>O<sub>3</sub>-Doped Si<sub>3</sub>N<sub>4</sub>," *J. Eur. Ceram. Soc.*, **19**, 227-37 (1999).

<sup>33</sup>S. M. Wiederhorn, D. E. Roberts, T.-J. Chuang, and L. Chuck, "Damage-Enhanced Creep in a Siliconized Silicon Carbide: Phenomenology," *J. Am. Ceram. Soc.*, **71**, 602-608 (1988).

<sup>34</sup>R. Morrell and K. H. G. Ashbee, "High-Temperature Creep of Lithium Zinc Silicate Glass-Ceramics, Part I, General Behaviour and Creep Mechanisms," *J. Mater. Sci.*, **8**, 1253-70 (1973).

<sup>35</sup>A. G. Robertson, D. S. Wilkinson, and C. H. Cáceres, "Creep and Creep Fracture in Hot-Pressed Alumina," *J. Am. Ceram. Soc.*, **74**, 915-21 (1991).

<sup>36</sup>R. F. Krause Jr., W. E. Luecke, and S. M. Wiederhorn, "Comparison of Tensile Creep Measurements on A Hot Isostatically Pressed Silicon Nitride," *J. Am. Ceram. Soc.*, in review.

<sup>37</sup>M. Gürtler and G. Grathwohl, "Tensile Creep of Sintered Silicon Nitride"; pp. 399-408 in *Creep and Fracture of Engineering Materials and Structures*.

Edited by B. Wilshire and R. W. Evans. The Institute of Metals, London, U.K., 1990.

<sup>38</sup>C.-F. Chen and T.-J. Chuang, "Improved Analysis for Flexural Creep with Application to Sialon Ceramics," *J. Am. Ceram. Soc.*, **73**, 2366-73 (1990).

<sup>39</sup>Q. Jin, X. G. Ning, D. S. Wilkinson, and G. C. Weatherly, "Compositional Dependence of Creep Behavior in Silicon Nitride Ceramics," *J. Can. Ceram. Soc.*, **65** [3] 211-14 (1996).

<sup>40</sup>F. Lange, B. I. Davis, and D. R. Clarke, "Compressive Creep of Si<sub>3</sub>N<sub>4</sub>/MgO Alloys, Part 1, Effect of Composition," *J. Mater. Sci.*, **15**, 601-10 (1980).

<sup>41</sup>J. Crampon, R. Duclos, and N. Rakotoharisoa, "Compression Creep of Si<sub>3</sub>N<sub>4</sub>/MgAl<sub>2</sub>O<sub>4</sub> Alloys," *J. Mater. Sci.*, **25**, 1203-208 (1990).

<sup>42</sup>J. Crampon, R. Duclos, and N. Rakotoharisoa, "Creep Behavior of Si<sub>3</sub>N<sub>4</sub>/Y<sub>2</sub>O<sub>3</sub>/Al<sub>2</sub>O<sub>3</sub>/AlN Alloys," *J. Mater. Sci.*, **28**, 909-16 (1993).

<sup>43</sup>S.-Y. Yoon, H. Kashimura, T. Akatsu, Y. Tanabe, S. Yamada, and E. Yasuda, "Grain Size Dependency on the Creep Rate in Hot-Pressed Silicon Nitride" (in Jpn), *J. Ceram. Soc. Jpn.*, **104** [10] 939-44 (1996).

<sup>44</sup>S. Yoon, T. Akatsu, and E. Yasuda, "Anisotropy of Creep Deformation Rate in Hot-Pressed Si<sub>3</sub>N<sub>4</sub> with Preferred Orientation of the Elongated Grains," *J. Mater. Sci.*, **32**, 3813-19 (1997).

<sup>45</sup>J. A. Schneider and A. K. Mukherjee, "Microstructural Evaluation of Deformation Mechanisms in Silicon Nitride Ceramics," *Ceram. Eng. Sci. Proc.*, **17** [3] 341-53 (1996).

<sup>46</sup>G. Bernard-Granger, J. Crampon, R. Duclos, and B. Cales, "High-Temperature Creep Behaviour of β'-Si<sub>3</sub>N<sub>4</sub>/α-Ysialon Ceramics," *J. Eur. Ceram. Soc.*, **17**, 1647-54 (1997).

<sup>47</sup>C. da Silva and T. J. Davies, "Compressive Creep of Silicon Nitride"; see Ref. 37, pp. 365-75.

<sup>48</sup>J. M. Birch and B. Wilshire, "The Compression Creep Behaviour of Silicon Nitride Ceramics," *J. Mater. Sci.*, **13**, 2627-36 (1978).

<sup>49</sup>J. Crampon, R. Duclos, F. Peni, S. Guicciardi, and G. De Portu, "Compressive Creep and Creep Failure of 8Y<sub>2</sub>O<sub>3</sub>/3Al<sub>2</sub>O<sub>3</sub>-Doped Hot-Pressed Silicon Nitride," *J. Am. Ceram. Soc.*, **80** [1] 85-91 (1997).

<sup>50</sup>P. J. Whalen, C. J. Gasdaska, and R. D. Silvers, "The Effect of Microstructure on the High-Temperature Deformation Behavior of Sintered Silicon Nitride," *Ceram. Eng. Sci. Proc.*, **11**, 633-40 (1990).

<sup>51</sup>M. S. Seltzer, "High-Temperature Creep of Silicon-Base Compounds," *Am. Ceram. Soc. Bull.*, **56**, 418-23 (1977).

<sup>52</sup>W. E. Luecke and J. S. Wallace, "Grain-Size Effects on Tensile Creep of Silicon Nitride," unpublished research, 1997.

<sup>53</sup>W. E. Luecke and J. D. French, "Sources of Strain Measurement Error in Flag-Based Extensometry," *J. Am. Ceram. Soc.*, **79** [6] 1617-26 (1996).

<sup>54</sup>M. K. Ferber; personal communication on cavities in PY-6 Si<sub>3</sub>N<sub>4</sub>, 1997.

<sup>55</sup>D. A. Koester, K. L. More, and R. F. Davis, "Deformation and Microstructural Changes in SiC-Whisker-Reinforced Si<sub>3</sub>N<sub>4</sub> Composites," *J. Mater. Res.*, **6**, 2735-46 (1991).

<sup>56</sup>T. Ohji and Y. Yamauchi, "Tensile Creep and Creep Rupture Behavior of Monolithic and SiC-Whisker-Reinforced Silicon Nitride Ceramics," *J. Am. Ceram. Soc.*, **76** [12] 3105-12 (1993).

<sup>57</sup>F. Lofaj, A. Okada, and H. Kawamoto, "Cavitation Strain Contribution to Tensile Creep in Vitreous-Bonded Ceramics," *J. Am. Ceram. Soc.*, **80** [6] 1619-23 (1997).

<sup>58</sup>T. Hirano, K. Niihara, T. Ohji, and F. Wakai, "Improved Creep Resistance of Si<sub>3</sub>N<sub>4</sub>/SiC Nanocomposites Fabricated from Amorphous Si-C-N Powder," *J. Mater. Sci. Lett.*, **15**, 505-507 (1996).

<sup>59</sup>D. Hull and D. E. Rimmer, "The Growth of Grain-Boundary Voids Under Stress," *Philos. Mag.*, **4**, 673-87 (1959).

<sup>60</sup>M. M. Chadwick and D. S. Wilkinson, "Microstructural Evolution in Annealed and Crept Silicon Nitride," *J. Am. Ceram. Soc.*, **76** [2] 376-84 (1993).

<sup>61</sup>K. Kussmaul, J. Helm, and S. Lauf, "Tensile Creep of Sintered Silicon Nitride Deformation Mechanisms and Lifetime Evaluation," *Key Eng. Mater.*, **89-91**, 635-40 (1994).

<sup>62</sup>S. U. Din and P. S. Nicholson, "Creep of Hot-Pressed Silicon Nitride," *J. Mater. Sci.*, **10**, 1375-80 (1975).

<sup>63</sup>K. J. Yoon, S. M. Wiederhorn, and W. E. Luecke, "A Comparison of Tensile and Compressive Creep Behavior in Silicon Nitride," *J. Am. Ceram. Soc.*, in review.

<sup>64</sup>T. W. Lambe and R. V. Whitman, *Soil Mechanics*. Wiley, New York, 1969.

<sup>65</sup>O. Reynolds, "On the Dilatancy of Media Composed of Rigid Particles in Contact with Experimental Illustrations"; pp. 203-16 in *Papers on Mechanical and Physical Subjects*, Vol. II. Cambridge University Press, Cambridge, U.K., 1901; reprinted from Dec. 1885 *Philosophical Magazine*.

<sup>66</sup>K. S. Chan and R. A. Page, "Creep Damage Development in Structural Ceramics," *J. Am. Ceram. Soc.*, **76**, 803-26 (1993).

<sup>67</sup>M. D. Thouless, "A Review of Creep Rupture in Materials Containing an Amorphous Phase," *Res. Mech.*, **22**, 213-42 (1987).

<sup>68</sup>A. G. Evans and A. Rana, "High-Temperature Failure Mechanisms in Ceramics," *Acta Metall.*, **28**, 129-41 (1980).

<sup>69</sup>R. L. Tsai and R. Raj, "Creep Fracture in Ceramics Containing Small Amounts of a Liquid Phase," *Acta Metall.*, **30**, 1043-58 (1982).

<sup>70</sup>M. D. Thouless and A. G. Evans, "Nucleation of Cavities During Creep of Liquid-Phase-Sintered Materials," *J. Am. Ceram. Soc.*, **67**, 721-27 (1984).

<sup>71</sup>R. Raj, "Nucleation of Cavities at Second-Phase Particles in Grain Boundaries," *Acta Metall.*, **26**, 995-1006 (1978).

<sup>72</sup>J. E. Marion, A. G. Evans, M. D. Drory, and D. R. Clarke, "High-Temperature Failure Initiation in Liquid-Phase-Sintered Materials," *Acta Metall.*, **31**, 1445-57 (1983).

<sup>73</sup>S. Suresh and J. R. Brockenbrough, "A Theory for Creep by Interfacial Flaw Growth in Ceramics and Ceramic Composites," *Acta Metall. Mater.*, **38** [1] 55-68 (1990).

- <sup>74</sup>J. A. Todd and Z.-Y. Xu, "The High-Temperature Creep Deformation of  $\text{Si}_3\text{N}_4\text{-}6\text{Y}_2\text{O}_3\text{-Al}_2\text{O}_3$ ," *J. Mater. Sci.*, **24**, 4443–52 (1989).
- <sup>75</sup>R. M. Arons and J. K. Tien, "Creep and Strain Recovery in Hot-Pressed Silicon Nitride," *J. Mater. Sci.*, **15**, 2046–58 (1980).
- <sup>76</sup>F. Lange, "Nonelastic Deformation of Polycrystals with a Liquid Boundary Phase"; pp. 361–81 in *Deformation of Ceramic Materials*. Edited by R. C. Bradt and R. E. Tressler. Plenum Press, New York, 1975.
- <sup>77</sup>B. F. Dyson, "Constraints on Diffusional Cavity Growth Rates," *Met. Sci.*, **10**, 349–53 (1976).
- <sup>78</sup>J. R. Dryden, D. Kucerovsky, D. S. Wilkinson, and D. F. Watt, "Creep Deformation Due to a Viscous Grain Boundary Phase," *Acta Metall.*, **37** [7] 2007–15 (1989).
- <sup>79</sup>J. R. Dryden and D. S. Wilkinson, "Three-Dimensional Analysis of the Creep Due to a Viscous Grain Boundary Phase," *Acta Mater.*, **45** [3] 1259–73 (1997).
- <sup>80</sup>M. M. Chadwick, D. S. Wilkinson, and J. R. Dryden, "Creep Due to a Non-Newtonian Grain-Boundary Phase," *J. Am. Ceram. Soc.*, **75**, 2327–34 (1992).
- <sup>81</sup>Q. Jin, X. G. Ning, D. S. Wilkinson, and G. C. Weatherly, "Redistribution of a Grain-Boundary Glass Phase during Creep of Silicon Nitride Ceramics," *J. Am. Ceram. Soc.*, **80** [3] 685–91 (1997).
- <sup>82</sup>N. Dey, K. J. Hsia, and D. F. Socie, "The Effects of Grain Size Distribution on Cavity Nucleation and Creep Deformation in Ceramics Containing Viscous Grain Boundary Phase," *Acta Mater.*, **45** [10] 4117–29 (1997).
- <sup>83</sup>S. M. Wiederhorn, W. E. Luecke, B. J. Hockey, and G. G. Long, "Creep Damage Mechanisms in  $\text{Si}_3\text{N}_4$ "; pp. 305–26 in Proceedings of the NATO Advanced Research Workshop, *Tailoring of Mechanical Properties of  $\text{Si}_3\text{N}_4$  Ceramics*. Edited by M. J. Hoffman and G. Petzow. Kluwer, Dordrecht, The Netherlands, 1994.
- <sup>84</sup>M. G. Jenkins, K. Breder, J. A. Salem, and V. J. Tennery, "Elevated-Temperature Macro-Flaw Fracture and Tensile Creep/Creep Rupture Behaviors of a Self-Reinforced Silicon Nitride"; pp. 257–67 in Ceramic Transactions, Vol. 42, *Silicon-Based Structural Ceramics*. Edited by B. W. Sheldon and S. C. Danforth. American Ceramic Society, Westerville, OH, 1994.
- <sup>85</sup>T. Ohji, Y. Yamauchi, and S. Kanzaki, "Tensile Creep and Creep Rupture Behavior of HIPed Silicon Nitride"; pp. 569–74 in *Proceedings of the International Conference on Silicon Nitride-Based Ceramics (Silicon Nitride 93)*. Edited by M. J. Hoffman, P. F. Becher, and G. Petzow. TransTech, Aedermannsdorf, Switzerland, 1994.
- <sup>86</sup>S. Haig, W. R. Cannon, P. J. Whalen, and R. G. Rateick, "Microstructural Effects on the Tensile Creep of Silicon Nitride"; pp. 91–96 in *Creep: Characterization, Damage, and Life Assessment*. Edited by D. A. Woodford, C. H. A. Townley, and M. Ohnami. ASM International, Materials Park, OH, 1992.
- <sup>87</sup>B. A. Fields and S. M. Wiederhorn, "Creep Cavitation in a Siliconized Silicon Carbide Tested in Tension and Flexure," *J. Am. Ceram. Soc.*, **79** [4] 977–86 (1996).
- <sup>88</sup>D. F. Carroll and R. E. Tressler, "Accumulation of Creep Damage in a Siliconized Silicon Carbide," *J. Am. Ceram. Soc.*, **71**, 472–77 (1988).
- <sup>89</sup>J. H. Li and D. R. Uhlmann, "The Flow of Glass at High Stress Levels, I. Non-Newtonian Behavior of Homogeneous  $0.08\text{Rb}_2\text{O}\text{-}0.92\text{SiO}_2$  Glasses," *J. Non-Cryst. Solids*, **3**, 127–47 (1970).
- <sup>90</sup>S. Webb, "Silicate Melts: Relaxation, Rheology, and the Glass Transition," *Rev. Geophys.*, **35** [2] 191–218 (1997).
- <sup>91</sup>S. L. Webb and D. B. Dingwell, "The Onset of Non-Newtonian Rheology of Silicate Melts," *Phys. Chem. Miner.*, **17**, 125–32 (1990).
- <sup>92</sup>D. C. Boyd and D. A. Thompson, "Glass"; p. 830 (Table 4) in Kirk-Othmer: Encyclopedia of Chemical Technology, Vol. 11. Wiley, New York, 1980.
- <sup>93</sup>G. Hetherington, K. H. Jack, and J. C. Kennedy, "The Viscosity of Vitreous Silica," *Phys. Chem. Glasses*, **5** [5] 130–36 (1964).
- <sup>94</sup>G. Hagen, "Ueber die Bewegung des Wassers in engen cylindrischen Röhren" (in Ger.), *Ann. Phys. Chem.*, **46**, 423–42 (1839).
- <sup>95</sup>J. L. Poiseuille, "Recherches Expérimentales sur le Mouvement des Liquides dans les Tubes de Très Petits Diamètres" (in Fr.), *C. R. Hebd. Seances Acad. Sci.*, **11**, 1041–48 (1840).
- <sup>96</sup>J. L. Poiseuille, "Recherches Expérimentales sur le Mouvement des Liquides dans les Tubes de Très Petits Diamètres" (in Fr.), *C. R. Hebd. Seances Acad. Sci.*, **12**, 112–15 (1841).
- <sup>97</sup>R. B. Bird, W. E. Stewart, and E. N. Lightfoot, *Transport Phenomena*. Wiley, New York, 1966.
- <sup>98</sup>P. C. Carman, "Fluid Flow through Granular Beds," *Trans. Inst. Chem. Eng.*, **15**, 150–61 (1937).
- <sup>99</sup>A. D. Krawitz, M. L. Crapenhoft, D. G. Reichel, and R. Warren, "Residual-Stress Distribution in Cermets," *Mater. Sci. Eng. A*, **A150/106**, 275–81 (1988).
- <sup>100</sup>A. D. Krawitz, D. G. Reichel, and R. L. Hitterman, "Residual-Stress Distribution in a WC–Ni Composite," *Mater. Sci. Eng. A*, **A119**, 127–34 (1989).
- <sup>101</sup>W. S. Kreher, "Modeling of Random Microstructural Stresses and Grain Boundary Damage in Polycrystals," *Comput. Mater. Sci.*, **7**, 147–53 (1996).
- <sup>102</sup>M. Abramowitz and I. A. Stegun, *Handbook of Mathematical Functions with Formulas, Graphs, and Mathematical Tables*, Applied Mathematical Series; p. 933, Eq. 26.2.24. U.S. Government Printing Office, Washington, DC, 1964.
- <sup>103</sup>G. D. Quinn, "Fracture Mechanism Maps for Advanced Structural Ceramics, Part I, Methodology and Hot-Pressed Silicon Nitride Results," *J. Mater. Sci.*, **25**, 4361–76 (1990).
- <sup>104</sup>S. Haig, W. R. Cannon, and P. J. Whalen, "Anelastic Recovery in Crept Silicon Nitride," *Ceram. Eng. Sci. Proc.*, **13** [9–10] 1008–23 (1992).
- <sup>105</sup>S. Haig, W. R. Cannon, and P. Whalen, "Tensile Creep, Recovery, and Failure of an *In Situ*-Reinforced Silicon Nitride," *J. Am. Ceram. Soc.*, in review.
- <sup>106</sup>J. D. French, S. M. Wiederhorn, and M. J. Hoffmann, "Grain Size Effects on Creep of Silicon Nitride," unpublished research, 1997.
- <sup>107</sup>M. J. Hoffmann, "High-Temperature Properties of Yb-Containing  $\text{Si}_3\text{N}_4$ "; see Ref. 83, pp. 59–72.
- <sup>108</sup>J. S. Vetrano, H.-J. Kleebe, E. Hampp, M. J. Hoffmann, M. Rühle, and R. M. Cannon, "Yb<sub>2</sub>O<sub>3</sub>-Fluxed Sintered Silicon Nitride, Part I, Microstructure Characterization," *J. Mater. Sci.*, **28**, 3529–38 (1993).
- <sup>109</sup>A. A. Wereszczak, T. P. Kirkland, and M. K. Ferber, "Stress and Strain Relaxation in HIPed Silicon Nitrides," *J. Mater. Sci. Lett.*, **13**, 1469–71 (1994). □